Available online at www.sciencedirect.com
ScienceDirect
Fuel 86 (2007) 1601–1613
FUEL
www.fuelfirst.com

Determination of multi-component gas and water equilibrium and non-equilibrium sorption isotherms in carbonaceous solids from early-time measurements

Hossein Jahediesfanjani *, Faruk Civan

Mewbourne School of Petroleum and Geological Engineering, The University of Oklahoma, Norman, OK 73019, USA

Received 22 October 2005; received in revised form 16 October 2006; accepted 2 November 2006
Available online 8 December 2006

Abstract

A rapid method is presented for determination of the multi-component gas and water sorption isotherms on carbonaceous solids from the non-equilibrium sorption data. This approach alleviates the long-time data requirement of the traditional volumetric gas adsorption technique used to construct gas isotherms requiring a series of equilibrium sorption measurements by successive pressure increments, particularly resorted in the coalbed methane industry. This is accomplished by the application of the non-equilibrium thermodynamics, multi-component material balance, gas sorption, and dissolution kinetic considerations for the gas adsorbed by carbonaceous solids and the gas dissolved in water under the effect of pressure, temperature, and grain size. The capabilities of the new technique in reducing the time required for construction of an isotherm are demonstrated by analyzing a series of the non-equilibrium sorption measurements and projecting the results to the equilibrium case. Moreover, it is demonstrated that the present model enables constructing both the equilibrium and non-equilibrium multi-component gas and water sorption isotherms in any carbonaceous solids and particularly coals simultaneously in relatively shorter time and with higher accuracy.

Keywords: Coalbed methane; Coal; ECGR

1. Introduction

Studying the simultaneous adsorption of water and multi-component gases in carbonaceous solids is important in the sorption industry in general and coalbed methane industry in particular. Coal is a mostly organic solid matter which can adsorb and store various gases in its pores. The amount of the adsorbed gas depends on the physical and chemical characteristics of the coal, gas, and water in contact with each other, and the prevailing pressure and temperature conditions. Presence of water in coalbed formations influences the ability of coal to adsorb and store various gases.

Kross et al. [1] report that moisture-equilibrated coals show lower methane adsorption capacity only about 20–25% compared to the dry coal. In general, the water in wet coalbed is present as a result of the chemical and physical bonding of coal and water, and influences the properties of the coal [2]. Gosiewska et al. [3] show that the mineralogical nature of coal largely influences the wettability of the coal surface with water. At macroscopic scale, carbon surface is hydrophilic adsorbing a little water [3]. However; the presence of the H-bonding sites at the coal surface may change the wettability and enhance water adsorption by forming strong bonds between the water molecules and the coal surface. In coalbed structure the gas is mostly adsorbed at the coal internal surface. Initially, the water, gas, and coal are at thermodynamic equilibrium [4,5].

There are several techniques to measure the sorption isotherm for a specific gas and solid matter. The volumetric

* Corresponding author. Tel.: +1 405 476 4585; fax: +1 405 325 7477.
E-mail address: hossein_j77@yahoo.com (H. Jahediesfanjani).

0016-2361/$ - see front matter © 2006 Elsevier Ltd. All rights reserved.
doi:10.1016/j.fuel.2006.11.019

Nomenclature

a	coal swelling coefficient (dimensionless)
b', c'	ratio of the liquid to the adsorbed phase density (dimensionless)
c, d	equilibrium isotherm fitting parameters (dimensionless)
D	D–A isotherm parameter (dimensionless)
D_o	the dissociation energy of the gas molecule $[M][L][T]^{-2}[Mol]^{-1}$
$\hat{f}$	fugacity $[M][T]^{-2}[L]^{-1}$
H	Henry's constant $[M][T]^{-2}[L]^{-1}$
j	net adsorption or solution rate $[T]^{-1}$
K	Boltzman constant, $1.38\times10^{-23}\ \frac{m^2\ kg}{T^2\ K}$
K'_{gs}	non-equilibrium constant for gas–water system $[T]^{-1}$
K_{gw}	non-equilibrium constant for gas–water system $[T]^{-1}$
Mw	molecular weight $[M][Mol]^{-1}$
P	pressure $[M][T]^{-2}[L]^{-1}$
P_c	critical pressure $[M][T]^{-2}[L]^{-1}$
r	D–A isotherm exponent (dimensionless)
R	universal gas constant $[M][L][T]^{-2}[Mol]^{-1}[K]$
R_a	adsorption rate $[L]^3[T]$
R_d	desorption rate $[L]^3[T]$
R_s	solution rate $[Mol][T]^{-1}$
R_{ds}	dissolution rate $[Mol][T]^{-1}$
T_c	critical temperature (K)
V	volume $[L]^3$
x	mole fraction of the component in liquid phase (dimensionless)
y	mole fraction of the component in gas phase (dimensionless)
z	gas compressibility factor (dimensionless)
ϕ	function of temperature and gas phase properties (dimensionless)
θ	ratio of the adsorbed volume to the maximum volume (dimensionless)
ρ	density $[M]\ [L]^{-3}$
γ	activity coefficient (dimensionless)
ω	gas component acentric factor (dimensionless)

Subscripts

a	adsorption
c	coal
d	desorption
e	equilibrium
f	final
G	gas component
g	gas phase
i, j	various components
s	solid
W	water component
w	water phase

technique is the most popular technique in the coalbed methane industry. Typically seven to ten measurements at different pressures are needed to construct an isotherm using this technique [6]. Sufficient time has to be allowed for each data points for the system to achieve equilibrium after each pressure reduction. Then, an appropriate isotherm is fitted to the data points. However, the constructed isotherm is based on the equilibrium measurements and does not represent the intermediate non-equilibrium conditions required for prediction of the gas production rates in actual coalbed gas production. Adsorption is a complicated process by which gas molecules under an applied pressure first approach the coal's internal pores and then they are adsorbed from the internal pore surfaces by the influence of the van der Waals attractive forces. The molecule adsorption continues until a thermodynamic equilibrium is obtained at the prevailing temperature and pressure conditions. This slow process can be described with an appropriate non-equilibrium sorption model.

The non-equilibrium adsorption models have been developed in the literature for the gas–liquid [7], solid–gas, and solid–liquid solutions [8]. The activated adsorption theory and Elovich equation are the two outstanding models used in the early adsorption kinetic studies [9]. Ward and Findlay [10] point out that the parameters of the activated adsorption theory are difficult to measure independently and the Elovich equation correlates the adsorption data better. They described the non-equilibrium adsorption model using the Elovich equation and the Langmuir isotherm. Lorenz and Engler [11] described the adsorption phenomenon by statistical thermodynamic. They found out that the adsorption energy or heat of adsorption change with the change in the amount of the adsorbed gas. Hamilton and Goodstein [12] presented a thermodynamic approach for the adsorption of methane on graphite surface. Do and Rice [13] considered the partial surface diffusion at non-equilibrium adsorption rates. Payne and Kreuzer [14] developed a non-equilibrium adsorption/desorption model using the quasi-chemical approximation and the sticking coefficient concept. The Langmuir model is based on considering that adsorption of a molecule into a mobile second layer takes place until gas molecules migrate to an empty site at the solid surface. In contrast, King [15] observed the presence of an intermediate state in the desorption kinetics. King concluded that ignoring the presence of the intermediate state could lead to serious errors in the derived values of the activated energy. Kreuzer and Payne [8] systematically formulated the rate equations controlling the time evolution of a two-phase adsorbate. They treated the two-dimensional (2D) gas as an ideal phase and described the two-dimensional condensate phase by Einstein's equation. Ward and Elmoselhi [16] predicted the net rate of the molecular

adsorption at a gas–solid interface and non-equilibrium adsorption using the statistical rate theory (SRT). The parameters of this model depend on the properties of the gas–solid surface conditions and are independent of the pressure and temperature conditions. Therefore, if such parameters are determined for a system of a gas and solid in the laboratory conditions they can be used in the SRT approach to predict the rate of adsorption in circumstances that are independent of the experimental conditions at which they were measured. This approach provides better results and predicts the adsorption phenomenon with higher accuracy than the activated adsorption theory and Elovich equation [17,18]. Rudzinsky and Panczyk [19] adopted the SRT with the Langmuir isotherm and developed non-equilibrium adsorption models to describe the volume-dominated, solid-dominated, and equilibrium-dominated cases. Rudzinsky and Panczyk [20] also introduced the statistical rate theory of interfacial transport (SRTIT) approach and developed the rate equation using the Dubinin and Astakhov (D–A) isotherm assuming that the gas fills the adsorption space in micropores via the mechanism of volume filling and hence not by forming a discrete monolayer. This model has been successful for applications to several carbonaceous and gaseous systems [21].

In the present study, the applications of the Statistical Rate Theory of Interfacial Transport (SRTIT) and the rate equation using the Dubinin and Astakhov (D–A) isotherm is extended for the multi-component gas and water adsorption on carbonaceous materials and coals by replacing the pressure with the equivalent fugacity and applying the modified Erying equation of state (EoS) to estimate the fugacity of the adsorbed phase in coal. The similar procedure is also used to model the time-dependency of the dissolution of various gases in water. The modified Peng–Robinson EoS, the modified UNIFAC-Lyngbe, and UNIFAC-Dortmund procedures are applied to predict the fugacity of the components in the gas and water phases. It is shown by analyzing typical experimental data that this model accurately predicts the volume of the various components of the coal, water, and gas phases contained in a closed PVT cell as a function of time. It is demonstrated that the non-equilibrium and equilibrium isotherms can be developed in a considerably shorter periods of time and with very high accuracy.

2. Formulation

A rapid interpretation procedure is developed for obtaining equilibrium and non-equilibrium isotherms from volumetric laboratory measurements. This model is based on the assumption that the gas/water adsorption on solid is the dominant process.

2.1. Overall material balance

Consider Fig. 1 describing the equipment composed of a constant volume PVT cell kept at a constant temperature

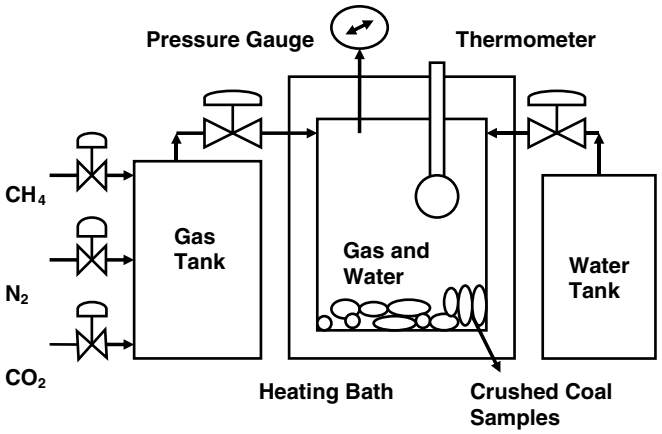

Fig. 1. The schematic scheme of the designed volumetric adsorption apparatus.

throughout the measurement. First, a certain volume of gas is charged into the PVT cell initially loaded with a certain amount of coal and water. The system is allowed sufficient time to attain an equilibrium at the initial pressure. As the gas and water adsorb on the coal, the composition and total pressure of the gas, water, and coal change in the PVT cell. The pressure variation in the PVT cell is recorded at various time steps until the equilibrium is reached.

The sum of the gas phase volume (V_g), water phase volume (V_w), and coal volume (V_c) is equal to the PVT-cell volume (V_{cell}) which remains constant while the volumes of the coal, water, and gas change with time. Hence, for a mixture below its critical pressure and temperature under the ideal conditions the following expression is true

$$V_{cell} = V_g(t) + V_c(t) + V_w(t) \tag{1}$$

where

$$V_w(t) = V_{Ww}(t) + V_{Gw}(t) \tag{2}$$

$$V_g(t) = V_{Gg}(t) + V_{Wg}(g) \tag{3}$$

The lower case subscript is a phase indicator and the upper case subscript represents the specific component contained in a phase. For instance, V_{Gw} refers to the volume of gas component in the water phase.

The relationships between the volume of each phase and its moles can be defined by

$$V_{Ww}(t) = \frac{n_{Ww}(t)\mathrm{Mw}_w}{\rho_{Ww}} \tag{4}$$

$$V_{Gw}(t) = \frac{n_{Gw}(t)\mathrm{Mw}_g}{\rho_{Gw}} \tag{5}$$

$$V_{Gc}(t) = \frac{n_{Gc}(t)\mathrm{Mw}_g}{\rho_{Gc}} \tag{6}$$

$$V_{Wg}(t) = \frac{n_{Wg}(t)\mathrm{Mw}_g}{\rho_{Wg}} \tag{7}$$

$$V_{Wc}(t) = \frac{n_{Wc}(t)\mathrm{Mw}_w}{\rho_{Wc}} \tag{8}$$

The mass conservation equations of the water and gas components are expressed as the following:

$$n_W = n_{Winitial} = n_{Wg}(t) + n_{Wc}(t) + n_{Ww}(t) \quad (9)$$

$$n_G = n_{Ginitial} = n_{Gw}(t) + n_{Gc}(t) + n_{Gg}(t) \quad (10)$$

Assuming a single component gas and low elevated pressure region (ideal mixture of single component gas and water) the average density of the gas phase is given by

$$\rho_{Gg}(t) = y_{Gg}\rho_{Gg}(t) + y_{Gw}\rho_{Gw}(t) \quad (11)$$

$$\rho_{Gg}(t) = \frac{n_{Gg}(t)}{n_{Gw}(t) + n_{Gg}(t)}\frac{Z_g RT}{P} + \frac{n_{Gw}(t)}{n_{Gw}(t) + n_{Ww}(t)}\frac{Z_w RT}{P} \quad (12)$$

$$\rho_{Gg}(t) = \rho_{Wg}(t) \quad (13)$$

$$\rho_{Ww}(t) = \frac{n_{Wg}(t)}{n_{Wg}(t) + n_{Ww}(t)}\frac{Z_g RT}{P} + \frac{n_{Ww}(t)}{n_{Wg}(t) + n_{Ww}(t)}\rho_w \quad (14)$$

The further step is to define the relationship necessary to calculate the density of the adsorbed phase inside the coal. The results of the analysis [22] of some fluids tested on many different carbonaceous solids show that the adsorbed phase density is very close to that of the liquid phase density at high pressure. Thus, the following expression for the density of the adsorbed phase can be written:

$$\rho_{Gc}(t) = b'\rho_{gL}(t) = b\frac{Z_{gL}RT}{P} \quad (15)$$

$$\rho_{Wc}(t) = c'\rho_{Wc}(t) = c\rho_{Ww}(P,T) \quad (16)$$

where b' and c' are the ratio of the adsorbed phase densities to density of the corresponding liquid phase at the prescribed pressure and temperature. The subscript L refers to the liquid phase. However, in reality the gas and water phases act as non-ideal phases. It will be explained later that the density of such mixtures is estimated using an appropriate equation of state.

2.2. Coal swelling

Maggs [23] assumed that the coal swelling is proportional to the heat of adsorption which is proportional to the system total pressure at a constant temperature. This assumption is approximately valid for gaseous hydrocarbon and nitrogen gas adsorption on coal [24]. Reucroft [25] reported the coal volume changes at various pressures and carbon content. Karacan [26] expressed the CO_2 swelling effects on coal very similarly to the water and liquid slurries. Thus, the coal swelling coefficient (c_c) can be used to estimate the coal volume change. The coal volume change due to adsorption of multi-component gases is assumed to be estimated as

$$\Delta V_c(t) = \sum_i [c_{ci}P_i] \quad (17)$$

where i refers to any adsorbed gas or water components.

2.3. Non-equilibrium gas sorption thermodynamic

At the initial reservoir condition the chemical potentials for the equilibrium gas, water, and coal system are equal. Thus,

$$\mu_{Gc} = \mu_{Wg} = \mu_{Gg} \quad (18)$$

$$\mu_{Wc} = \mu_{Wg} = \mu_{Ww} \quad (19)$$

Ward and Elmoselhi [16] used the Born–Oppenheimer approximation, the chemical potential per molecule of an ideal, asymmetric, and diatomic gas for the gas phase behavior. We use the general form of their expression for pure gas and under the ideal solution assumption given by

$$\mu_{gg} = kT\ln(y_{gg}P) \quad (20)$$

Similarly for water vapor in gas phase we have

$$\mu_{wg} = kT\ln(y_{wg}P) \quad (21)$$

Rudzinsky and Panczyk [20] described the net adsorption rate by the following kinetic equations.

$$J_{gc} = R_a - R_d \quad (22)$$

The adsorption and desorption rates are expressed by the SRIIT approach [17] as

$$R_a = K'_{gs}\exp\left(\frac{\mu_{Gc} - \mu_{Gg}}{kT}\right) \quad (23)$$

$$R_d = K'_{gs}\exp\left(\frac{\mu_{Gg} - \mu_{Gc}}{kT}\right) \quad (24)$$

where J_{gc} is the net gas exchange between the coal and gas phases.

Dubinin and Astakhov (D–A) (1971) developed an isotherm for adsorption of vapors on microporous adsorbents using Polany's theory of adsorption (1932) based on the physical and chemical concepts. The Dubinin and Radushkevich (D–R) and D–A isotherms are the semi-empirical relationships for adsorption of various gases and water vapors on coal surfaces, expressed as

$$\theta_i = \exp\left\{-\left[-D_i\ln\left(\frac{P_i}{P_0}\right)\right]^r\right\} \quad (25)$$

where r and D_i are the empirical values to be determined using the experimental data points. Eq. (25) is called D–R isotherm for $r = 2.0$ and D–A isotherm for other values of r. The value of r usually varies between 1.0 and 2.0 for carbons with large micropores [27]. However, the values less than 1.0 also have been reported for adsorption of gases on the activated carbons [20]. Using the D–A isotherm and substituting Eqs. (23)–(25) into Eq. (22) and integrating using the initial condition of $\theta\ (t = 0) = 0.0$, yields

$$\theta_i(t) = \exp\left\{-\left[-D_i\ln\frac{P_i}{P_0}\tanh(2PK_{gsi}t)\right]^r\right\} \quad (26)$$

2.4. Non-equilibrium gas–water thermodynamics

The following equations similar to those given above can also be written for the gas-water system as

$$J_{gw} = R_{ds} - R_s \tag{27}$$

$$R_{ds} = K_{gw} \exp\left(\frac{\mu_{Gg} - \mu_{Gw}}{kT}\right) \tag{28}$$

$$R_s = K_{gw} \exp\left(\frac{\mu_{Gw} - \mu_{Gg}}{kT}\right) \tag{29}$$

$$\mu_{Gg} = kT \ln(Py_{Gg}) \tag{30}$$

$$\mu_{Gw} = kT \ln(H_{Gw} x_{Gw}) \tag{31}$$

Substituting Eqs. (33)–(36) into Eq. (32) yields

$$\frac{dy_{Gg}}{dt} = K_{gw}\left(\frac{Py_{Gg}}{H_{Gw}x_{Gw}} - \frac{H_{Gw}x_{Gw}}{Py_{Wg}}\right) \tag{32}$$

$$\frac{dx_{Gw}}{dt} = K_{gw}\left(\frac{H_{Gw}x_{Gw}}{Py_{Gw}} - \frac{Py_{Gg}}{H_{Gw}x_{Gw}}\right) \tag{33}$$

Eqs. (32) and (33) are subject to the following initial conditions and the auxiliary equations:

$$x_{Gw}(t=0) = 0 \quad \text{and} \quad y_{Wg}(t=0) = 0$$

$$\sum_{i=1}^{n} y_i = 1 \quad \text{and} \quad \sum_{i=1}^{n} x_i = 1$$

This procedure can be extended readily for the multi-component gas and water adsorption on the coal surface. Multi-component adsorption is the case that the gas phase is composed of more than one component. Therefore, the gas and adsorbed mixtures deviate from the ideal mixture state. To account for these deviations, the pressure (P) in Eqs. (20)–(31) is substituted by fugacity ($\hat{f}_{g_i g}$). Therefore, Eqs. (26), (32), and (33) become

$$\theta_{G_i c}(t) = \exp\left\{-\left[-D_{g_i} \ln\frac{\hat{f}_{G_i g}}{P_0} \tanh(2\hat{f}_{G_i g} K_{gsi} t)\right]^r\right\} \tag{34}$$

$$\frac{dy_{G_i g}}{dt} = K_{g_i w}\left(\frac{\hat{f}_{G_i g}}{\hat{f}_{G_i w}} - \frac{\hat{f}_{G_i w}}{\hat{f}_{G_i g}}\right) \tag{35}$$

$$\frac{dx_{Gw}}{dt} = K_{gw}\left(\frac{\hat{f}_{G_i w}}{\hat{f}_{G_i g}} - \frac{\hat{f}_{G_i g}}{\hat{f}_{G_i w}}\right) \tag{36}$$

2.5. Fugacity calculations

The fugacity of any component in the gas phase can be estimated using the Peng–Robinson [29] equation of state:

$$\ln\left(\frac{\hat{f}_{G_i g}}{y_{G_i g} P}\right) = \frac{b_k}{b}(Z-1) - \ln(Z-B) - \frac{A}{2\sqrt{2}B}\left(\frac{2\sum_i y_{G_i g} a_{G_k g}}{a} - \frac{b_k}{b}\right) \ln\left(\frac{Z + 2.414B}{Z - 0.414B}\right) \tag{37}$$

where

$$Z^3 - (1-B)Z^2 + (A - 3B^2 - 2B)Z - (AB - B^2 - B^3) = 0 \tag{38}$$

$$a = \sum_i \sum_j y_{G_i g} y_{G_j g} a_{ij} \tag{39}$$

$$b = \sum_i y_{G_i g} b_i \tag{40}$$

$$a_{ij} = (1 - \delta_{ij}) a_i^{1/2} a_j^{1/2} \tag{41}$$

$$a = 0.45724 \frac{R^2 T_c^2}{P_c} \sqrt{1 + k(\omega)(1 - T_r^{1/2})} \tag{42}$$

$$b = 0.07780 \frac{RT_c}{P_c} \tag{43}$$

$$k(\omega) = 0.37464 + 1.54226\omega - 0.26992\omega^2 \tag{44}$$

$$A = \frac{aP}{R^2 T^2}; \quad B = \frac{bP}{RT} \tag{45}$$

The fugacity of the components in water phase is calculated by [28,29,31]

$$\ln\left(\frac{\hat{f}_{G_i w}}{x_{G_i w}}\right) = \ln(\gamma_{G_i w} H^{\circ}_{i,w}) + \frac{\bar{v}_{G_i w}}{RT}(P - P^{sat}_w) \tag{46}$$

$$\ln\left(\frac{\hat{f}_{Ww}}{x_{Ww}}\right) = \ln(\gamma_{Ww} \phi^{sat}_{Ww} P^{sat}_{Ww}) + \frac{v^{sat}_{Ww}}{RT}(P - P^{sat}_{Ww}) \tag{47}$$

where $\gamma_{G_i w}$ is the activity of the gas component i in water phase and $\gamma_{W_i w}$ is activity coefficient of the water component in the water phase. The activity coefficients are calculated using the modified UNIFAC-Lyngby [30,32] and UNIFAC-Dortmond [30,34] correlations.

Degance [36] modified the Erying EoS for multi-component adsorption of various gas component mixtures on coal by accounting for the binary interaction coefficients. This representation is used to estimate the fugacity of the components at the adsorbed phase as

$$\ln(A\hat{f}_{G_i c}) - \ln(RT) = \ln\tilde{\omega}_{g_i c} - 2\ln(1 - \sqrt{\beta\tilde{\omega}}) + \frac{2\sum\beta_{ij}\tilde{\omega}_j - \beta\tilde{\omega}}{\sqrt{\beta\tilde{\omega}}(1 - \sqrt{\beta\tilde{\omega}})} - \frac{2}{RT}\sum_j \alpha_{ij}\tilde{\omega}_j \tag{48}$$

where

$$\alpha_{ij} = (1 - k^{\alpha}_{ij})\sqrt{\alpha_i \alpha_j} \quad \text{and} \quad \beta_{ij} = (1 - k^{\beta}_{ij})\sqrt{\beta_i \beta_j} \tag{49}$$

$$\tilde{\omega} = \sum \tilde{\omega}_i \text{ and } \beta\tilde{\omega}^2 = \sum\sum \beta_{ij}\tilde{\omega}_i\tilde{\omega}_j \tag{50}$$

where $\tilde{\omega}_i$ is the adsorbed moles of component i over the mass of the adsorbent. β_i and α_i are the Erying EoS constants for component i. We determined these constants for various coal, water, methane, nitrogen, and carbon dioxide systems at different temperature ranges using a trial-and-error method in a manner to minimize the difference between the right and left hand sides of Eq. (48). Table 1 summarizes the references and limitations considered to obtain the constant parameter values [32–36]. The corresponding values for the binary interaction coefficients between components i and j (k_{ij}) for water, methane, nitro-

Table 1
Conditions of the coal and gas system case obtained from the literature considered to estimate α and β

Coal	Gas mixture	Temperature (K)	Pressure (MPa)	Reference #
Dry AC-F400	N_2, CH_4, CO_2	319	0.35–11.8	42
Wet Fruitland	N_2, CH_4, CO_2	318	0.35–11.8	42
Wet Tiffany	N_2, CH_4, CO_2	328	0.35–11.8	42
High Vitrinite C-3.2 B-11	CH_4, CO_2	300–330	0.10–13.88	43
Low Vitrinite B2-10 D3-7	CH_4, CO_2	300–330	0.10–13.88	43
Wyoming Char	H_2O	Ambient	$P/P_0 < 0.6$	44
Yallourn–Briquette char	H_2O	Ambient	$P/P_0 < 0.6$	44
Bituminous coal No. 6	H_2O	Ambient	$P/P_0 < 0.6$	45
Bituminous coal No. 956	H_2O	Ambient	$P/P_0 < 0.6$	45
Anthracite No. 1	H_2O	Ambient	$P/P_0 < 0.6$	45
High rank bituminous	H_2O	Ambient	$P/P_0 < 0.6$	46
Low rank bituminous	H_2O	Ambient	$P/P_0 < 0.6$	46

gen, and carbon dioxide in the adsorbed phase are presented elsewhere [33,37]. Therefore, Eqs. (48)–(50) can be generally used to estimate the fugacity values of the adsorbed components of water, nitrogen, carbon dioxide, and methane on various coal–gas mixture systems.

3. Determination of non-equilibrium isotherms

A computer code was developed in MATLAB to solve the above equations and calculate the amount of each gas component in the water, gas, and coal phases. The calculation procedure is as following:

1. Measure the initial solid, gas, water volumes, and their component mole fractions.
2. Monitor the pressure changes as a function of time.
3. Calculate the values of P_0 for various gas components using the method proposed with Kapoor [42].
4. Guess new gas and water phase component mole fractions for both gas and water phases.
5. Estimate the gas phase components fugacity using Eqs. (37)–(45) and water phase activity coefficients using Eqs. (46) and (47).
6. Calculate the gas and water phase component mole fractions using Eq. (51) (a convenient form of Eqs. (35) and (36)).

$$m_{G_i g}^{t+1} = \Delta t \cdot K_{gw_i} \left(\frac{\hat{f}_{g_i g}}{\hat{f}_{g_i w}} - \frac{\hat{f}_{g_i w}}{\hat{f}_{g_i g}} \right) + m_{g_i g}^{t} \tag{51}$$

where m represents y for gas phase and x for liquid phase and t represents the time step.

7. Compare the calculated x and y with the assumed values in step 4. If the difference is sufficiently small, then move to step 8, otherwise repeat steps 5–7 using the just calculated values of x and y.
8. Use the overall material balance Eqs. (1)–(12) to calculate the volume of the adsorbed gas components and calculate the mole fraction of each component in the coal.
9. Estimate the fugacity of the adsorbed phase using Eqs. (48)–(50) and Table 1.
10. Plot $\ln(V_i)$ versus $X = \left\{ -\ln\left[\frac{\hat{f}_{g_i c}}{P_0} \tanh(2\hat{f}_{g_i c} K_{gsi} t) \right] \right\}^r$ according to Eq. (52) (a convenient form of Eq. (34)), and fit the best curve to the data points and determine the parameters of D, r, K_{gs} and V_m for each component.

$$\ln V_i = \ln V_{mi} - D_i^r \left\{ -\ln\left[\frac{\hat{f}_{g_i c}}{P_0} \tanh(2\hat{f}_{g_i c} K_{gsi} t) \right] \right\}^r \tag{52}$$

Therefore, the non-equilibrium isotherm in the form of Eq. (52) is constructed. However, the rate of adsorption/desorption and the parameters of Eq. (53) may be functions of the total pressure, temperature, and grain size of the coal particles in a given system of gas, solid, and water. Therefore, Eq. (53) can be rewritten in a general form as

$$\ln V_i = \ln[G_{V_{mi}}(\hat{f}_{g_i c}, d, T)] - [G_{D_i}(\hat{f}_{g_i c}, d, T)]^{[G_r(\hat{f}_{g_i c}, d, T)]} \times \left\{ -\ln\left[\frac{\hat{f}_{g_i c}}{P_0} \tanh(2\hat{f}_{g_i c} G_{K_{gsi}}(\hat{f}_{g_i c}, d, T) t) \right] \right\}^{G_r(\hat{f}_{g_i c}, d, T)} \tag{53}$$

where G represents a series of empirical relationships for the parameters of V_m, D, r, and K_{gsi} as functions of fugacity (pressure), grain size, and temperature. It is demonstrated later that the parameters r and K_{gsi} have constant values, the parameter V_m has a logarithmic relationship with the component fugacity and the grain size, and D is a linear function of the grain size and component fugacity.

4. Verification and applications

The applications of the above mentioned technique are presented to construct the equilibrium and non-equilibrium isotherms rapidly and with high quality for prediction of the primary coalbed methane production and the enhanced recovery by CO_2 and N_2 injection into the coalbeds.

4.1. Obtaining equilibrium and non-equilibrium isotherms

The examples presented here utilize the non-equilibrium data points to establish both equilibrium and non-equilibrium isotherms.

4.1.1. Scenario 1. Pure methane, carbon dioxide, and nitrogen adsorption on coal

Gasem et al. [43] reported pure methane, carbon dioxide, and nitrogen adsorption rate data on the Tiffany coal. Fig. 2 shows the procedure of curve fitting of the data points using Eq. (52) for various values of r at three different pressures (1.39, 4.85, and 10.4 MPa). Tables 2–5 represent the best-estimate values for r, k, D, P_0, and V_m for the system of methane, carbon dioxide, and nitrogen on coal at these pressures. As can be seen, the value of r and k are independent of pressure and are only functions of the gas and carbonaceous material properties. P_0 is only a function of temperature and gas properties, D and V_m are both functions of pressure. The maximum theoretical gas adsorption volume (V_m) according to Fig. 3 has a logarithmic relationship with pressure that can be described as

$$G_{V_m}(P) = a_{V_m} \ln P + b_{V_m} \tag{54}$$

However, D (the D–R coefficient) according to Fig. 4 has a linear relationship with pressure, described as

$$G_D(P) = a_D P + b_D \tag{55}$$

The value of D used in D–A and D–R equations is considered to be only a property of the adsorbent (coal) [20]. However, Fig. 3 shows that pressure variation can affect

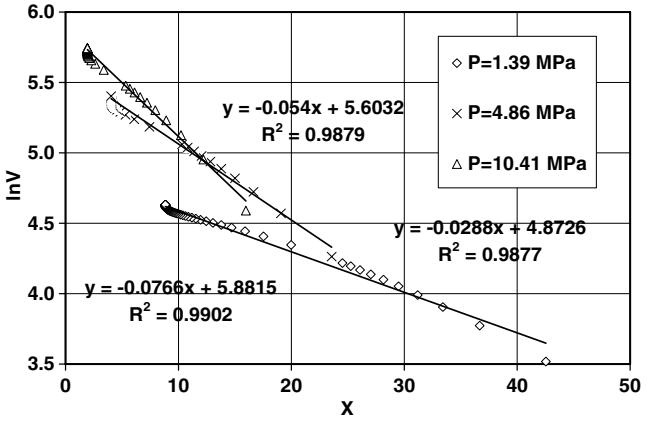

Fig. 2. Procedure of obtaining the equilibrium isotherm for different pressures.

Table 2
Best-estimated values of the parameters for CH_4 non-equilibrium isotherm on coal calculated in this study

P (MPa)	r	P_0 (MPa)	k	ln V_m	D^r	V_m	D
1.38	1.75	44.5	0.000016	1.31	0.029	3.70	0.132
3.45	1.75	44.5	0.000016	1.86	0.046	6.40	0.171
4.83	1.75	44.5	0.000016	2.04	0.054	7.70	0.189
6.21	1.75	44.5	0.000016	2.13	0.057	8.50	0.194
7.58	1.75	44.5	0.000016	2.20	0.059	9.06	0.198
8.96	1.75	44.5	0.000016	2.30	0.077	9.90	0.23
10.34	1.75	44.5	0.000016	2.31	0.081	10.13	0.237

Table 3
Best-estimated values of the parameters for CH_4 non-equilibrium isotherm on coal (well#10) calculated in this study

P	r	P_0	k	ln V_m	D^r	V_m	D
1.38	1.9	44.5	0.00013	1.73	0.021	5.63	0.130
3.45	1.9	44.5	0.00013	2.17	0.038	8.77	0.178
4.83	1.9	44.5	0.00013	2.30	0.046	9.90	0.198
6.21	1.9	44.5	0.00013	2.38	0.051	10.81	0.209
7.58	1.9	44.5	0.00013	2.44	0.056	11.52	0.219
8.96	1.9	44.5	0.00013	2.48	0.073	12.0	0.252
10.34	1.9	44.5	0.00013	2.52	0.076	12.45	0.258

Table 4
Best-estimated values of the parameters for CO_2 non-equilibrium isotherm on coal calculated in this study

P	r	P_0	k	ln V_m	D^r	V_m	D
1.38	1.9	20.7	0.000018	2.14	0.020	8.49	0.126
3.45	1.9	20.7	0.000018	2.51	0.044	12.82	0.193
4.83	1.9	20.7	0.000018	2.60	0.056	13.52	0.220
6.21	1.9	20.7	0.000018	2.70	0.068	14.43	0.244
7.58	1.9	20.7	0.000018	2.71	0.081	15.071	0.266
8.96	1.9	20.7	0.000018	2.72	0.103	15.31	0.303
10.34	1.9	20.7	0.000018	2.74	0.105	15.66	0.306

Table 5
Best-estimated values of the parameters for N_2 non-equilibrium isotherm on coal calculated in this study

P	r	P_0	k	ln V_m	D^r	V_m	D
1.38	1.0	15.86	0.000068	1.10	0.040	3.00	0.040
3.45	1.0	15.86	0.000068	1.27	0.053	3.57	0.053
4.83	1.0	15.86	0.000068	1.53	0.060	4.62	0.060
6.21	1.0	15.86	0.000068	1.68	0.058	5.38	0.058
7.58	1.0	15.86	0.000068	1.79	0.062	6.00	0.062
8.96	1.0	15.86	0.000068	1.86	0.074	6.42	0.074
10.34	1.0	15.86	0.000068	1.92	0.071	6.82	0.071

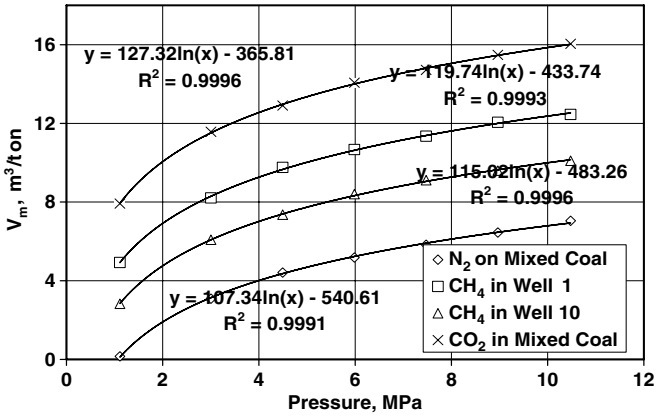

Fig. 3. Relationship between values of V_m and pressure for methane, carbon dioxide and nitrogen adsorption on coal.

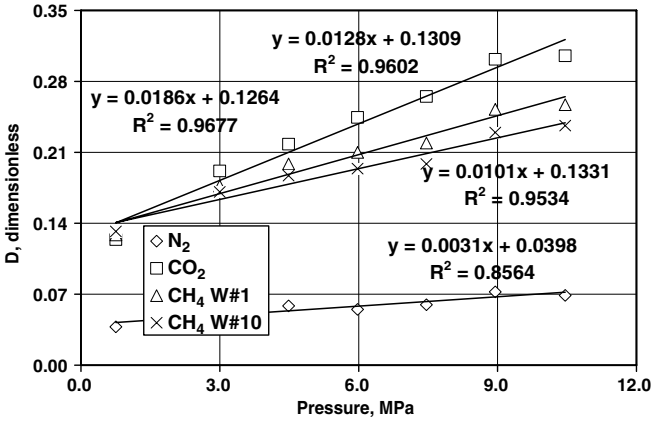

Fig. 4. Relationship between values of D and pressure for methane, carbon dioxide and nitrogen adsorption on coal.

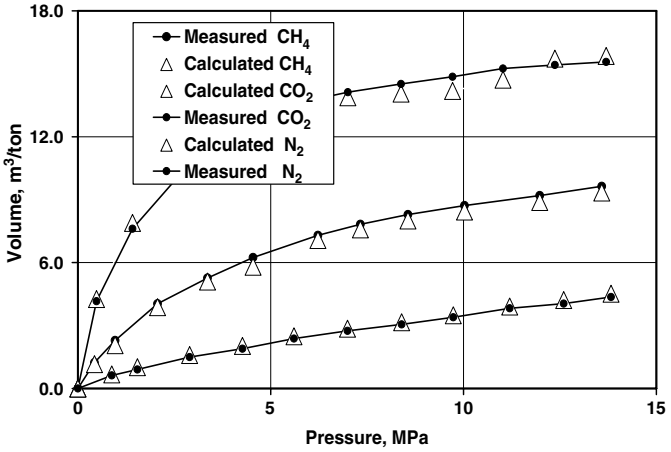

Fig. 5. Measured and predicted equilibrium isotherms for methane, carbon dioxide and nitrogen in tiffany coal.

the value of D. Therefore, the properties of the adsorbent (coal) itself changes as the pressure and type of the gas in contact with the coal changes. In fact, Larsen [22] concluded that gas solution in coal changes the coal properties to some extend depending upon the type of the gas and coal. Larsen points out that the dissolved carbon dioxide in coal acts as a plasticizer enabling a structure rearrangement so that the second adsorption of CO_2 is subject to the same coal with different structure. Fig. 4 shows that value of D varies with pressure for carbon dioxide more than methane and nitrogen. Moreover, the rate of the change for carbon dioxide is faster than methane and nitrogen because the carbon dioxide is adsorbed preferentially more on coal than the other gases. Eq. (43) can be rewritten as

$$\ln V_i = [a_{V_m} \ln(\widehat{f}_{g_i g}) + b_{V_m}] - (a_D \widehat{f}_{g_i g} + b_D)^r \times \left\{ -\ln\left[\frac{\widehat{f}_{g_i c}}{P_0} \tanh(2\widehat{f}_{g_i c} K_{gsi} t) \right] \right\}^r \quad (56)$$

This equation provides a non-equilibrium isotherm for adsorption of any gas on carbonaceous materials. The equilibrium isotherm can be obtained in the limit by applying

$$\lim_{t\to\infty} \tanh(2\widehat{f}_{g_i c} k_{gsi} t) = 1.0 \quad (57)$$

Therefore, a non-equilibrium equation can be transformed to equilibrium isotherm as

$$\ln V_i = [a_{V_m} \ln(\widehat{f}_{g_i c}) + b_{V_m}] - (a_D \widehat{f}_{g_i c} + b_D)^r \left[-\ln\left(\frac{\widehat{f}_{g_i c}}{P_0} \right) \right]^r \quad (58)$$

Eq. (58) is the modified D–R isotherm for the case of high pressure and multi-component gas adsorption on the coal. Fig. 5 compares the measured and calculated equilibrium isotherms for methane, carbon dioxide, and nitrogen using the Gasem [43] data. The difference between the two isotherms is less than 3%. This exercise illustrates that both non-equilibrium and equilibrium isotherms can be obtained from the same type of the measurements performed to obtain the equilibrium isotherms using this method.

Given the values of the D_e and V_{me} coefficients for equilibrium isotherm a non-equilibrium isotherm can be constructed for the same system using the following relationship:

$$D_{ie} = \frac{\int_{\widehat{f}_{in}}^{\widehat{f}_f} [a_{Di}(\widehat{f}_{g_i c}) + b_{Di}] d\widehat{f}}{\Delta \widehat{f}} \quad (59)$$

$$D_{ie} = \frac{a_{Di}(\widehat{f}^2_{g_i cf} - \widehat{f}^2_{g_i c_{in}})}{2(\hat{f}_{g_i cf} - \hat{f}_{g_i c_{in}})} + b_{Di} \quad (60)$$

$$V_{mie} = \frac{\int (a_{V_{mi}} \ln \widehat{f}_{g_i c_f} + b_{Vmi}) d\hat{f}_{g_i c}}{\widehat{f}_{g_i c_f} - \widehat{f}_{g_i c_{in}}} \quad (61)$$

$$V_{mie} = \frac{a_{Vmi}}{\widehat{f}^2_{g_i c_f} - \widehat{f}^2_{g_i c_{in}}} + b_{Vmi} \quad (62)$$

Substituting Eqs. (59) and (60) into Eq. (58) and rearranging yield

$$\ln V_i = a_{Vmi} \left\{ \left[\ln(\hat{f}_{g_i c}) - \frac{1}{\hat{f}^2_{g_i cf} - \hat{f}^2_{g_i cin}} + \frac{V_{mie}}{a_{Di}} \right] - \left(\frac{a_{Di}}{a_{Vmi}} \right)^r \times \left[\hat{f}_{g_i c} - \frac{\hat{f}_{g_i cf} - \hat{f}_{g_i cf}}{2} + \frac{D_{ie}}{a_{Di}} \right]^r \left[\ln\left(\frac{\hat{f}_{g_i c}}{P_0} \right) \right]^r \right\} \quad (63)$$

A plot of the right hand side versus the left hand side of Eq. (63) results in a straight line with a slope of a_{Vmi}. The best straight line is obtained by adjusting the values of a_{Di} and a_{Vmi}. These values are used in Eqs. (60) and (61) to estimate the values of b_{Di} and b_{Vmi}. Therefore, Eq. (58) describes a non-equilibrium isotherm constructed using an equilibrium isotherm.

4.1.2. Scenario 2. Dependency of the kinetic parameters to coal particle size distribution

Busch et al. [44] reported several experimental rate data on the adsorption of methane and carbon dioxide in Silesia

Table 6
Best-estimated values of the parameters for CH_4 non-equilibrium isotherm on Sileca coal for various grain sizes

d_g (mm)	r	P_0 (MPa)	k	$\ln V_m$	D^r	V_m	D
<0.063	3.0	29.47	0.000006	4.27	0.0032	71.27	0.147
0.063–0.15	3.0	29.47	0.000006	3.93	0.003	51.22	0.144
0.15–3.0	3.0	29.47	0.000006	3.76	0.0029	42.56	0.1426
>3.0	3.0	29.47	0.000006	3.74	0.0023	40.64	0.132

Table 7
Best-estimated values of the parameters for CO_2 non-equilibrium isotherm on Sileca coal for various grain sizes

d_g(mm)	r	P_0	k	$\ln V_m$	D^r	V_m	D
<0.063	1.0	20.68	0.001	5.36	1.52	211.70	1.52
0.063–0.15	1.0	20.68	0.001	5.00	1.41	146.20	1.46
0.15–3.0	1.0	20.68	0.001	4.56	1.37	95.11	1.39
>3.0	1.0	20.68	0.001	4.05	1.301	57.67	1.15

315 coal for different grain sizes ranging from grains diameters less than 0.063 to higher than 3.0 mm. Their data indicate different times to reach equilibrium for different grain sizes. The rate of adsorption is faster for smaller particles than the bigger ones. Therefore, the particle size affects the non-equilibrium isotherm parameters. Tables 6 and 7 show the best estimate values of the parameters obtained by matching the Eq. (51) with Busch et al. [44] adsorption kinetic data. As can be seen, the values of D and V_m decrease as the particles size increases. Figs. 6 and 7 show that V_m has a logarithmic relationship with the grain size, whereas D varies linearly with the particle diameter. In coalbed reservoirs, the coal matrix is composed of the grains in different sizes and combinations. Given the grain size distribution, the effect of the grain size on non-equilibrium isotherm and adsorption/desorption rates in the real reservoir condition can be considered in construction of the correct non-equilibrium and equilibrium isotherms using

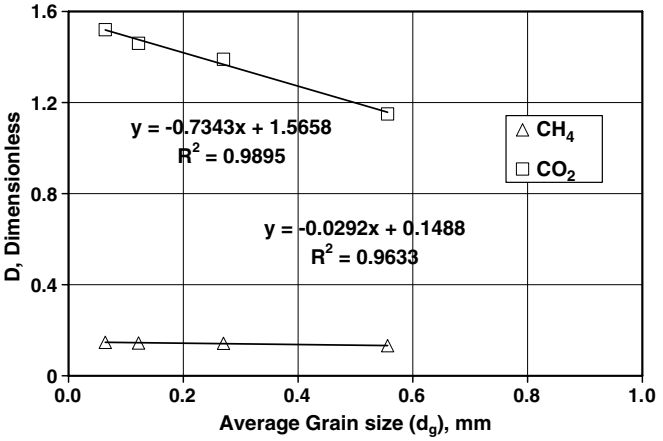

Fig. 7. The linear relationship between parameter D and average coal grain size.

$$G_{\overline{D}_A}(d) = \frac{\int_0^A [a_{\mathrm{dD}} f(d) + b_{\mathrm{dD}}]\mathrm{d}A}{\int_0^A \mathrm{d}A} \tag{64}$$

$$G_{\overline{V}_{mA}}(d) = \frac{\int_0^A \{a_{\mathrm{d}V_m} \ln[f(d)] + b_{\mathrm{d}V_m}\}\mathrm{d}A}{\int_0^A \mathrm{d}A} \tag{65}$$

where $f(d)$ is the grain size distribution function over coal surface area (A).

4.1.3. Scenario 3. Water adsorption on various coals

The equilibrium and non-equilibrium water adsorption experimental data are reported in the literature for several coals. The equilibrium data points are usually better fitted with D–R and D–A isotherms at lower relative pressures ($P/P_0 < 0.6$) [38] and BET isotherm at higher relative pressures [40]. However, the non-equilibrium sorption data on coal show very similar trend as the gas sorption data on coal. Examining several water sorption kinetic data [38–41] reveals that the non-equilibrium isotherm developed in this study can be used to model the intermediate time-dependent water adsorption data. Figs. 8 and 9 show the

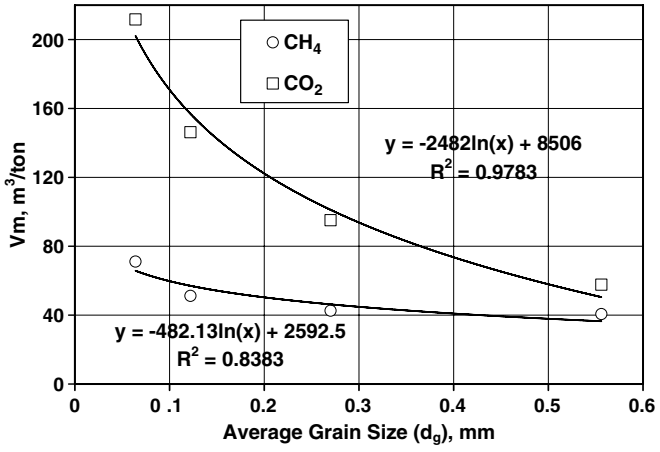

Fig. 6. The logarithmic relationship between the maximum coal gas adsorbed volume and average coal grain size.

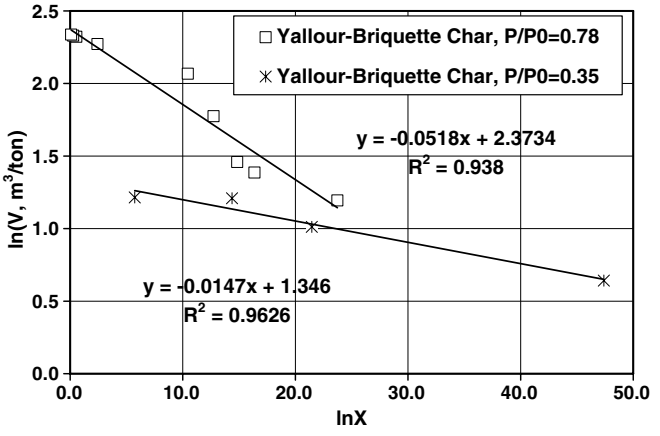

Fig. 8. Model fitting of water adsorption on Yallourn–Briquette charcoal with various relative pressures.

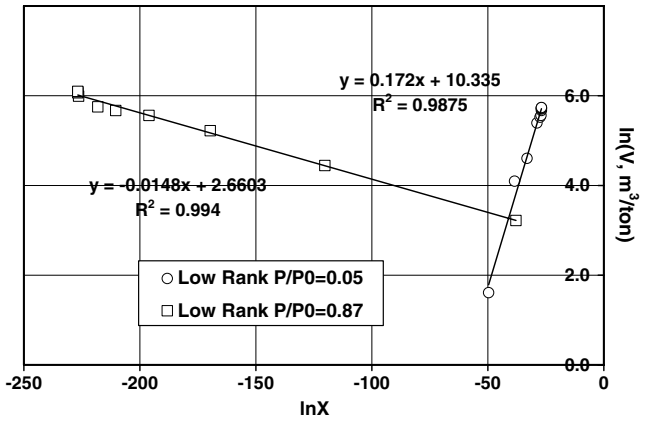

Fig. 9. Model fitting of water adsorption on low rank coal with various relative pressures.

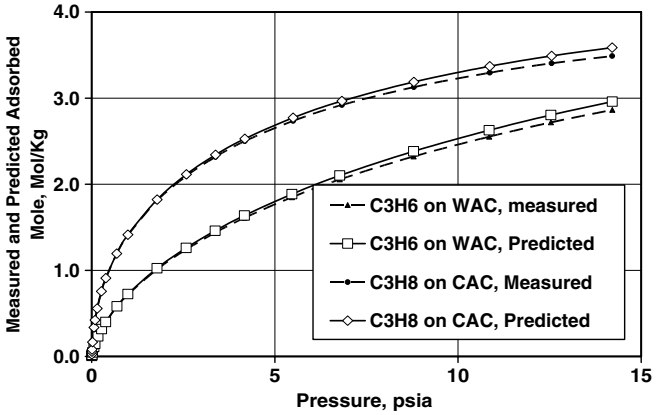

Fig. 10. Comparison of the predicted and measured [51] equilibrium isotherms for propane and propylene adsorption on activated carbons.

fit of the water adsorption kinetic data using the present model. The data fitting error (difference between the measured and the calculated data points) is about 1–5%. This is considered a good match between the predicted and the measured values.

4.1.4. Scenario 4. Propane and propylene adsorption on Chemviron and Wesvaco activated carbon at low pressures

The present computer code uses reported measured non-equilibrium adsorption data points for adsorption of propane and propylene on commercial activated carbons and regenerates the equilibrium adsorption isotherms for each component [46]. Fig. 10 presents the comparison between measured and predicted isotherms. As can be seen, the average error is less than 2%.

4.1.5. Scenario 5. Pure methane adsorption on carbon molecular sieves

The methane and other gas adsorption data on carbon molecular sieves are reported in the literature. [44] Following the steps 2–4 and using the equilibrium and non-equilibrium data reported in reference [44] the equilibrium and non-equilibrium isotherm parameters are determined for each gas component. Table 8 summarizes the values obtained from steps 2–4. Fig. 11 shows a plot of Eq. (31) required to predict the mentioned parameters for methane. Similarly, the same set of plots can be developed for other gases. This figure is constructed for different values of r in a fixed value of K_{gs}. To determine the value of r we take into account that this value is usually between 0.1 and 2.0 for adsorption of different gases on carbonaceous materials. Therefore, any value of r in this range should result with a better straight line fit. To improve the value of R^2, parameter K_{gs} is varied until the best possible fit is obtained for the reported data. The slope of the straight line is equal to D^r that is used to estimate the value of D. The intercept is equal to $\ln V_m$ that is used to estimate the value of V_m. Now that the non-equilibrium isotherm is established, the parameters of Eqs. (54) and (55) can be determined yielding the most general form of the non-equilibrium isotherm corresponding to Eq. (56). Fig. 12 presents the non-equilibrium methane adsorption isotherms on the carbon molecular sieves at different pressures. Fig. 13 compares the predicted and measured equilibrium data points. According to this figure, the points are very close to each other and the error is less than 8%.

Table 8
Best-estimated non-equilibrium isotherm parameters for various gases

Parameter gas comp.	r	D	V_m	a	B
CH_4	0.3	0.025	19.30	2.60	24.14
C_2H_6	0.3	0.020	25.64	1.747	10.171
CO_2	1.3	0.017	105.24	4.14	5.51
C_3H_8	0.2	0.019	46.13	1.21	4.34
N_2	0.2	0.024	208.8	4.6	3.23

4.1.6. Scenario 6. Mixture of methane, ethane and carbon dioxide adsorption on carbon molecular sieves

The gas mixture contains 95% CH_4, 3% CO_2, and 2% C_2H_6. A volume of 160 cm^3 gas mixture is injected into a PVT-cell of 130 cm^3 size at the initial condition of 75 °F

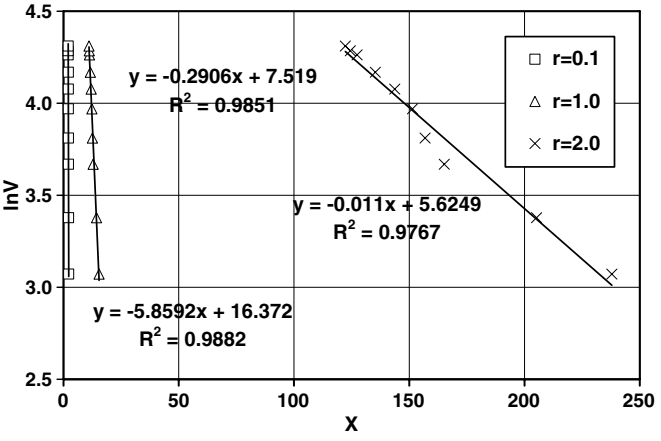

Fig. 11. Adsorbed methane volume vs. X explained in step 10.

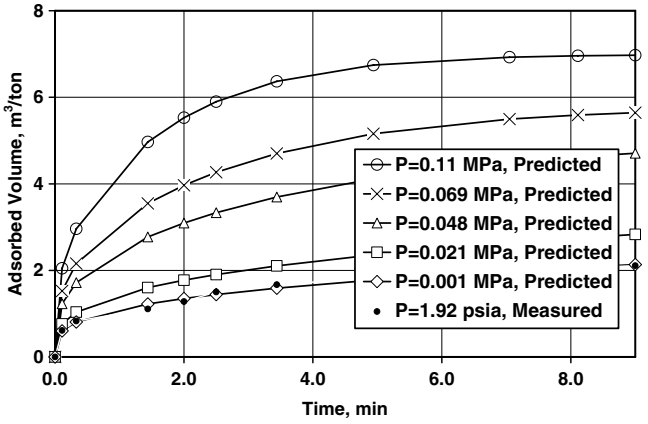

Fig. 12. Measured and predicted non-equilibrium isotherm for adsorption of methane on molecular sieve surface at various pressures.

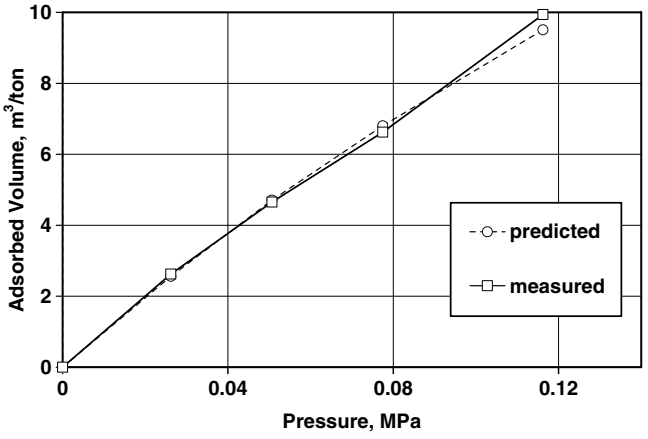

Fig. 13. Comparison of the measured and predicted equilibrium data with the estimated values using the non-equilibrium isotherm parameters.

and 100 K Pa. The developed model constructs the equilibrium and non-equilibrium isotherms for various pressures using the estimated parameters reported in Table 8 and the compressibility values for various gases [22]. Figs. 14–16 present the non-equilibrium isotherms for the projected high pressures using the reported low-pressure values for methane, carbon dioxide, and ethane, respectively. Fig. 17 shows the relationship between methane, carbon dioxide, and ethane mole fractions in the gas phase and the adsorbed volume in the coal phase. Ethane adsorbs faster than carbon dioxide and methane.

4.2. Discussion of the model assumptions and limitations

Modeling the non-equilibrium water and multi-component gas adsorption on coal is a very challenging task. This study presented a solution to estimate the adsorbed amount of multi-component gas and water in coal simultaneously based on several assumptions. The assumptions are unavoidable as a part of each model. The developed model in this study was tested using several literature data.

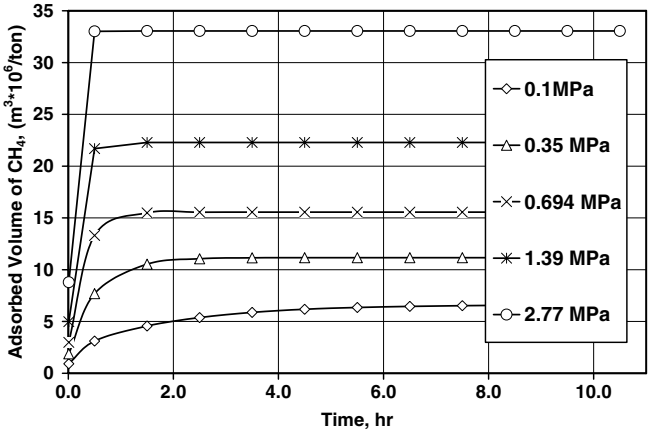

Fig. 14. Prediction of the CH_4 non-equilibrium adsorption isotherms for the higher pressures.

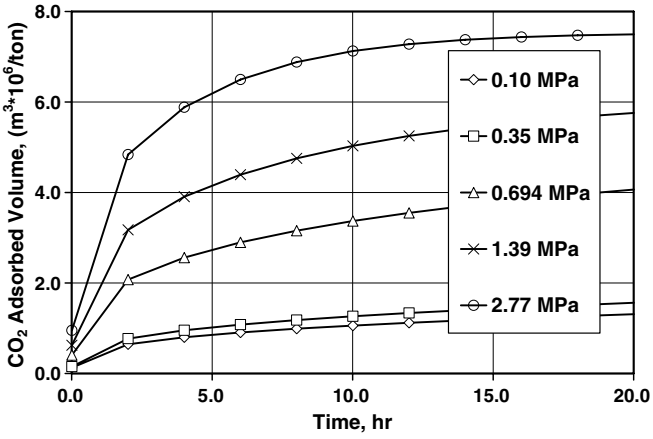

Fig. 15. Prediction of the CO_2 non-equilibrium adsorption isotherms for the higher pressures.

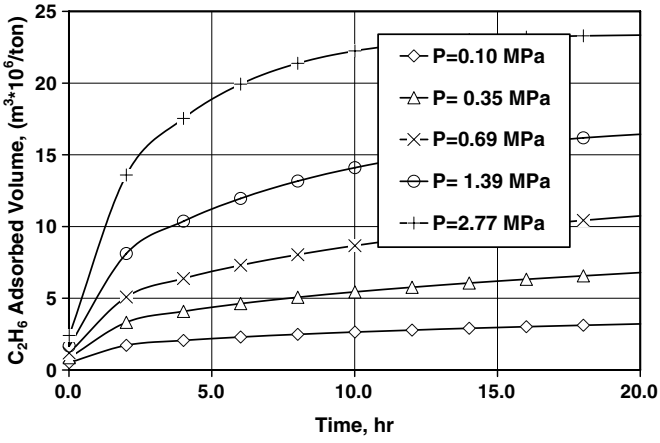

Fig. 16. Prediction of the C_2H_6 non-equilibrium adsorption isotherms for the higher pressures.

Therefore, to validate some specific features of our model, we had to use the other relevant experimental data such as adsorption of gases on molecular sieves, activated carbons

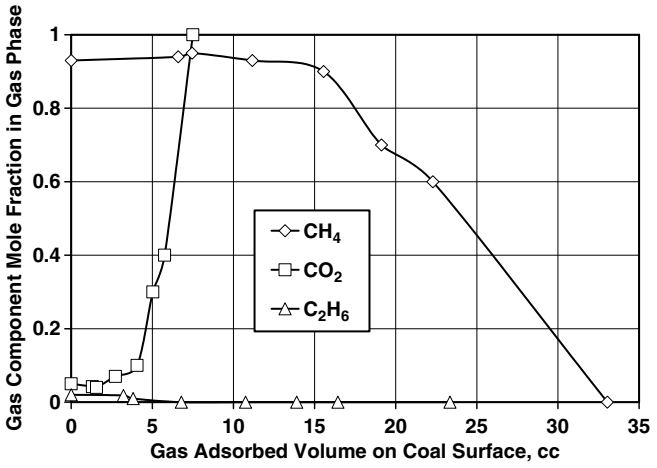

Fig. 17. Predicted gas mole fractions in gas phase vs. the gas adsorbed volume in coal.

and so on. The origin and source of most of these artificial adsorbents is coal. Therefore, we believe validating some features of our model using these sorts of data would be appropriate. It is important to emphasize that the sorption system may have different features that determines its energy level. We did not underestimate this fact. However, it is beyond the scope of this study to investigate various scenarios, for instance, the cases in which coal swelling or gas activated diffusion is the limiting process. The current study focused only on the adsorption of various gases and water in coal. This phenomenon was modeled using the chemical potential concept. In fact, the intensive attempts at modeling the kinetics of adsorption started by Polany's simple model in late 1890s and resulted in one of the latest models describing the kinetics of adsorption introduced and confirmed by Rudzinsky and Panczyk based on the statistical rate theory of interfacial transport (SRTIT). We, in fact, applied the SRTIT model and extended it for the multi-component and multi-phase sorption scenarios. We hope that this study opens the door for further investigation.

5. Conclusions

This study presented and validated the formulations required for the development of the non-equilibrium, multi-component, and three phase sorption model under certain assumptions. The various scenarios presented in this study demonstrated that the overall non-equilibrium and equilibrium isotherms can be constructed for all pressure and grain size ranges with very high accuracy (less than 5% prediction error) and in a considerably shorter time period (less than 1/10th of the regular time) if only two sets of the intermediate non-equilibrium sorption data points for two pressure levels are available. The model parameters are adjusted to account for the effects of solid grain sizes and applied pressure levels. A full curve fitting procedure is introduced to obtain model parameters using the non-equilibrium experimental sorption data. The developed model has been proven to be applicable for prediction of the adsorption of single and multi-component gases on various carbonaceous solids.

Another advantage of this model is the ability of modeling the water–coal–gas internal interactions. This was implemented by a model based on the chemical potential driving forces differences between three phases of solid, water, and multi-component gas. Considering that the coalbed methane reservoirs usually contain the three phases of coal, gas, and water in contact with each other, our model leads to more realistic results in compared to the two phase gas-coal models.

Appendix A. Supplementary data

Supplementary data associated with this article can be found, in the online version, at doi:10.1016/j.fuel.2006.11.019.

References

[1] Krooss BM, Bergen F, Gensterblum Y, Siemons N, Pagnier HJM, David P, et al. High-pressure methane and carbon dioxide adsorption on dry and moisture-equilibrated Pennsylvanian coals. Int J Coal Geol 2002;51:69–92.
[2] Snyder GT, Riese WCR, Franks S, Pelzmann WL, Gorody AW, Moran JE, et al. Origin and history of waters associated with coalbed methane: ^{129}I, ^{36}Cl, and stable isotope resulting from the fruitland formation, CO and NM. J Geochim Cosmochim Acta 2003;67(23):4529–44.
[3] Gosiewska A, Drelich J, Laskowski JS, Pawlik M. Mineral matter distribution on coal surface and its effect on coal wettability. J Colloid Interf Sci 2002;247:107–16.
[4] Jahediesfanjani H, Civan F. Damage tolerance of well-completion and stimulation techniques in coalbed methane reservoirs. J Energy Res Technol 2005;127:1–9.
[5] Jahediesfanjani H, Civan F. Productivity of fractured and non-fractured horizontal wells in coalbed methane reservoirs. In: Paper 521, the 2005 international coalbed methane symposium, Tuscaloosa, Alabama, 10–12 May, USA; 2005.
[6] Mavor MJ, Owen LB, Terra Tek Inc, Pratt T. Measurement and evaluation of coal sorption isotherm data. In: Proceedings from the SPE annual technical conference and exhibition, 23–26 September, New Orleans, LA; 1990.
[7] Ward CA. The rate of gas adsorption at a liquid interface. J Chem Phys 1977;67(1):229–35.
[8] Kreuzr HJ, Payne SH. Non-equilibrium thermodynamics of a two-phase adsorbate. Surface Sci 1988;198:235–62.
[9] Low MJD. Kinetics of chemisorption of gases on solids. Chem Reviews 1960;60:276–312.
[10] Ward CA, Findlay RD. Statistical rate theory of interfacial transport. III. Predicted rate of non-dissociative adsorption. J Chem Phys 1982;76(11):5615–23.
[11] Lorenz W, Engler C. Chemisorption with partial charge transfer on semiconductor surfaces: adsorption equilibrium and adsorption isotherm. Surface Sci 1984;114:607–13.
[12] Hamilton JJ, Goodstein DL. Thermodynamic study of methane multilayer adsorbed on graphite. J Phys Review B 1983;28(7):3838–48.
[13] Do DD, Rice RG. On the relative importance of pore and surface diffusion in non-equilibrium adsorption rate processes. J Chem Eng Sci 1987;42(10):2269–84.

[14] Payne SH, Kreuzer HJ. Analysis of thermal desorption data. Surface Sci 1989;222:404–29.
[15] King DA. The influence of weakly bound intermediate states on thermal desorption kinetics. Surface Sci 1977;64:431–51.
[16] Ward CA, Elmoselhi M. Molecular Adsorption at a Well Defined Gas-Solid Interphase: Statistical Rate Theory approach. Surface Sci 1986;176:457–75.
[17] Elliot JAW, Ward CA. Statistical rate theory desorption of beam-dosing adsorption kinetics. J Chem Phys 1997;106(13):5667–77.
[18] Elliot JAW, Ward CA. Temperature programmed desorption: a statistical rate theory approach. J Chem Phys 1997;106(13):5678–84.
[19] Rudzinski W, Panczyk T. The Langmuirian adsorption kinetics revised: a farewell to the XXth century theories? Fuel 2000:1963–74.
[20] Rudzinski W, Panczyk T. Kinetics of gas adsorption in activated carbons, studied by applying the statistical rate theory of interfacial transport. J Phys Chem B 2001;105:6858–66.
[21] Jahediesfanjani H, Civan F. Rapid determination of equilibrium gas isotherms in wet coalbeds from non-equilibrium state measurements. In: Paper 521, the 2005 international coalbed methane symposium, May 10–12, Tuscaloosa, AL, USA; 2005.
[22] Vyas SN, Patwardhan SR, Vijayalakshimi S, Ganesh KS. Adsorption of gases on carbon molecular sieves. J Colloid Interf Sci 1994;168:275–80.
[23] Maggs FAP. The adsorption–swelling of several carbonaceous solids. Trans Faraday Soc 1946;42B:284–8.
[24] Larsen JW. The effects of dissolved CO_2 on coal structure and properties. Int J Coal Geol 2004;57:63–70.
[25] Reucroft PJ, Sethuraman AR. Effect of pressure on carbon dioxide induced coal swelling. Energy Fuels 1987;1:72–5.
[26] Karacan CO. Heterogeneous sorption and swelling in a confined and stressed coal during CO_2 injection. Energy Fuels 2003;17:1595–608.
[27] Clarkson CR. Application of a new multi-component gas adsorption model to coal gas adsorption systems. Soc Petrol Eng J 2003:236–51.
[28] Apol MEF, Amadei A, Berendsen HJC. Application of quasi-Guassian entropy theory to the calculation of thermodynamic properties of water and methane in the liquid and gas phase. J Phy Chem 1996;104(17):6666–78.
[29] Peng DY, Robinson DB. A new two-constant equation of state. Ind Eng Chem, Fundam 1976;15(1):59–64.
[30] Evelein KA, Moore RG. Prediction of phase equilibria in sour natural gas systems using the Soave–Redlich-known equation of state. Ind Eng Chem Process Des Dev 1979;18(4):618–24.
[31] Mohammadi AH, Chapoy A, Tohidi B, Richon D. Water content measurement and modeling in the nitrogen–water system. J Chem Eng Data 2005;50:541–5.
[32] Weidlich U, Gmehling J. A modified UNIFAC Model. 1. Prediction of VLE, h^E and the activity coefficients at infinite dilution. Ind Chem Res 1987;26:1327–81.
[33] Li J, Vanderbeken I, Ye S, Carrier H, Xans P. Prediction of the solubility of gas–liquid equilibria for gas–water and light hydrocarbon-water systems at high temperatures and pressures with a group contribution equation of state. Fluid Phase Equilibria 1997;131:107–18.
[34] Larsen BL, Rasmussen P, Fredenslund A. A modified UNIFAC group contribution model for the prediction of phase equilibria and heats of mixing. Ind Eng Chem Res 1987;26:2274–86.
[35] Dhima A, de Hampinne JC, Jacques J. Solubility of hydrocarbons and CO_2 mixtures in water under high pressure. Ind Eng Chem Res 1999;38:3144–61.
[36] DeGance AE. Multicomponent high-pressure adsorption equilibria on carbon substrates: theory and data. Fluid Phase Equilib 1992;78:99–137.
[37] Sudibandriyo M, Pna Z, Fitzgerald JE, Robinson RL, Gasem KAM. Adsorption of methane, nitrogen, carbon dioxide, and their binary mixtures on dry activated carbon at 318.2 K and pressures up to 13.6 MPa. Langmuir 2003;19:5323–31.
[38] Clarkson CR, Bustin RM. Binary gas adsorption/desorption isotherms: effect of moisture and coal composition upon carbon dioxide selectivity over methane. Int J Coal Geol 2000;42:241–71.
[39] Monazam ER. Water adsorption and desorption by coals and chars. Energy Fuels 1998;12:1299–304.
[40] Mahajan OP, Walker PL. Water adsorption on coal. Fuel 1971;50(3):308–17.
[41] McCutcheon AL, Barton WA, Wilson MA. Kinetics of water adsorption/desorption on bituminous coals. Energy Fuels 2001;15: 1387–95.
[42] Kapoor A, Ritter JA, Yang RT. On the Dubinin–Radushkevich equation for adsorption in microporous solids in the Henry's law region. Langmuir 1989;5:1118–21.
[43] Gasem KAM, Robinson RL, Reeves SR. Adsorption of pure methane, nitrogen, and carbon dioxide and their mixtures on san juan basin coal. In: A topical report contract no#DE-FC26-00NT40924, Oklahoma State University, May; 2002.
[44] Busch A, Gensteblum Y, kross BM, Littke R. Methane and carbon dioxide-diffusion experiments on coal: upscaling and modeling. Int J Coal Geol 2004;60:151–68.
[45] Allardice DJ, Evans DG. The brown coal/water system: Part 2. Water sorption isotherm on bed-moist Yallourn brown coal. Fuel 1971;50(3):236–53.
[46] Mofarahi M, Sadrameli M, Towfighi J. Characterization of activated carbon by propane and propylene adsorption. J Chem Eng Data 2003;48(5):1256–61.